Aging aware adaptive control of Li-ion battery energy storage system for flexibility services provision

Chethan Parthasarathy, Hannu Laaksonen, Eduardo Redondo-Iglesias, Serge Pelissier

Journal of Energy Storage 57 (2023) 106268

Contents lists available at ScienceDirect

Journal of Energy Storage

journal homepage: www.elsevier.com/locate/est

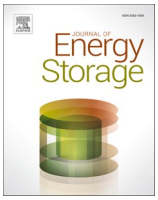

Research papers

Aging aware adaptive control of Li-ion battery energy storage system for flexibility services provision

Chethan Parthasarathy [a,*], Hannu Laaksonen [a], Eduardo Redondo-Iglesias [b], Serge Pelissier [b]

[a] Flexible Energy Resources, Electrical Engineering, University of Vaasa, Vaasa, Finland
[b] LICIT-ECO7 Lab, Univ Eiffel, ENTPE, Univ Lyon, Bron, France

ARTICLE INFO

Keywords:
Lithium ion battery
Battery aging characterisation
Power system control and modelling
Active network management

ABSTRACT

Battery energy storage systems (BESSs) play a major role as flexible energy resource (FER) in active network management (ANM) schemes by bridging gaps between non-concurrent renewable energy sources (RES)-based power generation and demand in the medium-voltage (MV) and low-voltage (LV) electricity distribution networks. However, Lithium-ion battery energy storage systems (Li-ion BESS) are prone to aging resulting in decreasing performance, particularly its reduced peak power output and capacity. BESS controllers when employed for providing technical ancillary i.e. flexibility services to distribution (e.g. through ANM) or transmission networks must be aware of changing battery characteristics due to aging. Particularly of importance is BESSs' peak power changes aiding in protection of the Li-ion BESS by restricting its operation limits of it for safety reasons and improving its lifetime in the long run. In this paper, firstly an architecture for ANM scheme is designed considering Li-ion BESSs as one of the FERs in an existing smart grid pilot (Sundom Smart Grid, SSG) in Vaasa, Finland. Further, Li-ion BESS controllers are designed to be adaptive in nature to include its aging characteristics, i.e. tracking the changing peak power as the aging parameter, when utilised for ANM operation in the power grid. Peak power capability of the Li-ion nickel-manganese-cobalt (NMC) chemistry-based battery cell has been calculated with the experimental data gathered from accelerated aging tests performed in the laboratory. Impact of such aging aware and adaptive Li-ion BESS controllers on the flexibility services provision for power system operators needs will be analysed by means of real-time simulation studies in an existing SSG pilot.

1. Introduction

Modern power systems landscape is changing rapidly in order to facilitate reduction on fossil fuel utilization and tackle climate change issues. This has led to large and rapid integration of renewable energy sources (RES) in medium voltage (MV) and low voltage (LV) distribution networks. One of the major issues in RES integration, arises from their intermittency in power generation which causes fluctuation in system parameters such as its frequency and voltage [1,2].

Active network management (ANM) provides an opportunity for efficient management of the flexible energy sources (FERs) for flexibility services provision for distribution system operators (DSOs) increasing needs related, for example, to voltage fluctuations [3,4]. FERs play an essential role by offering multiple different flexibility services for DSOs as well as for transmission system operators (TSOs). They provide ways for improved existing network capacity utilization without excessive passive network component upgrades and simultaneously more reliable and efficient network operation. In the development of future-proof ANM methods FER controllers play a major role. For example, inverter-based resources such wind turbine generators are capable of participating in flexibility services provision by its reactive power control dependent on local voltage target value or simultaneous active power output. However, flexibility services feasible provision requires design of suitable controllers for different purposes (flexibility service needs).

Inverter-based BESSs can be seen as ideal flexibility services providers due to their potential and versatility in providing multiple active (P) and reactive power (Q) related flexibility services for different DSO and TSO needs like, for example, for voltage and frequency control, black start, islanding, load leveling and peak shaving [5,6]. Thereby, BESSs are very useful for bridging gap between non-concurrent RES-based power generation and demand at different voltage (U) levels of the power system.

Recently, Li-ion battery energy storage systems (Li-ion BESSs) have become the forefront choice for utilization in land-based grid support

* Corresponding author.
E-mail address: chethan.parthasarathy@uwasa.fi (C. Parthasarathy).

https://doi.org/10.1016/j.est.2022.106268
Received 18 May 2022; Received in revised form 24 October 2022; Accepted 26 November 2022
Available online 5 December 2022

Nomenclature

BESS	battery energy storage systems
FER	flexible energy resources
ANM	active network management
RES	renewable energy sources
LV	low voltage
MV	medium voltage
NMC	Nickel-Managenese-cobalt battery chemistry
TSO	transmission system operator
SOH	state of health
SOC	state of charge
SSG	sundom smart grid
DER	distributed energy resources
DSO	distribution system operator
EMS	energy management system
WTG	wind turbine generator
BMS	battery management system
PP	peak power
HPPC	hybrid pulse power characterisation test
SEI	solid electrolye interface
CCCV	constant current constant voltage
CC	constant current
DOD	depth of discharge
SOEC	second order equivalent circuit
P_{dis}	battery active power discharge
P_{chg}	battery active power charge
P_{Load}	total load power
P_{WT}	wind turbine active power generation
$P_{BESS,\ REF}$	Li-ion BESS active power reference without age consideration
SOC_{min}	SOC minimum limits
SOC_{max}	SOC maximum limits
$P_{CELL,\ REF}$	Li-ion battery cell reference without age consideration
Ns	number of battery cells in series
Np	number of battery cells in parallel
P_{cell}	battery cell power
$P_{CELL,\ REF,\ age}$	Li-ion battery cell reference without age consideration
$SOC_{initial}$	initial battery SOC
I_{cell}	current per cell
Q_{wind}	reactive power contribution from WTG
Q_{ref}	reactive power reference
$Q_{wind,\ av}$	available reactive power from WTG
Q_{BESS}	reactive power contribution from Li-ion BESS
R_{dis}	DC discharge resistance of battery cell
PP_{Dis}	peak power during battery cell discharge
R_{cha}	DC charge resistance of battery cell
PP_{cha}	peak power during battery cell charge
$P_{BESS,\ REF,\ age}$	Li-ion BESS active power reference with age consideration

applications, by acting as a FER which is capable of providing multiple flexibility services for ANM operations in the distribution system [7]. Nowadays, Li-ion BESSs are commercially available for large-scale for grid applications with power ratings in the range of hundreds of MWs. The power and energy density, lower self-discharge, slow aging rates, improved safety and high modularity in their construction are some of the reasons behind adoption of Li-ion batteries for grid applications [8].

However, performance of Li-ion BESSs are affected by various parameters such as depth of discharge (DOD), state of charge (SOC), temperature and aging [9]. Further, performance degradation due to aging, mainly leads to change in battery capacity and their peak power capability. This peak power changes in Li-ion BESS is a function of its SOC and aging. This means that the Li-ion BESS peak power output will differ for a new battery compared to a wear and tear induced cycled BESS. Hence, the design for controllers of Li-ion BESS, especially for their secondary and tertiary control must include aging parameter as an input, i.e., in this case its evolving peak power capability. Failure to do so might accelerate the overall aging process and may lead to fatality due to internal short circuits, especially when expected peak power can no longer be offered by the Li-ion BESSs, which shall happen particularly when the battery is nearing its end of life.

In existing control related studies in literature, Li-ion BESSs have been used extensively. For example, in [10] Li-ion BESS has been utilised to develop a test model for various grid related control studies and the battery model in this study was developed based on equivalent circuit model with SOC, C-rate and temperature as affecting parameters. A fuzzy logic based coupling of voltage and frequency control was established for BESS in [11]. The control design also considered battery's state of health (SOH) (an empirical model) to define control parameters, but considered capacity loss with SOC and DOD as affecting parameters. Distributed secondary control for a multi-BESS distribution system was proposed in [12] where the objective was to compensate deviations introduced by droop control and improve SOC balancing among multiple BESS units, without considering battery aging effects.

In existing literature, most of the studies related to battery modelling and control concentrate on long-term cost-based optimization techniques [13–18]. Some of the recent studies [19–21] have also utilised battery aging models, i.e., their capacity degradation and resistance increase as aging parameters in the power system planning and control studies (predominantly considered as the tertiary control of microgrids). However, the literature focused on real-time design of BESSs' (e.g. Li-ion BESS) secondary control have not paid attention on their aging characteristics [22–25]. Further, according to authors' best knowledge, the peak power evolution of the Li-ion battery with aging has not been considered as an aging parameter in any of the studies presented in the previous literature. According to the authors' experience in analyzing field data from battery utilization, majority of the battery load in the secondary control has higher power requirement and DOD when compared to primary control. Therefore, it is important to include state of age (SOA), i.e., number of operational charge/discharge cycles completed is considered as SOA in this study and its corresponding peak power capability of the Li-ion BESS in the secondary control design.

Therefore, the scope of this paper is as follows,

1. Development of ANM architecture with *QU*-, *PU*- and *P*-controllers for managing available flexibilities of various distributed energy resources (DER), especially to generate control signals for the inverters of the Li-ion BESS and wind turbine generator (WTG) connected in the MV distribution network.
2. Primary focus has been on the development of Li-ion BESS *P*-control for ANM functionality related to active power dispatch control in which battery utilization in terms of age calculation in number of cycles of charge/discharge completed is also considered. In addition, *P*-control is designed to supply charge/discharge power within the battery's peak (active) power capability.
3. In order to develop *P*-control for ANM, accurate equivalent circuit battery model and peak power evolution model for Li-ion BESS has been developed in detail. These are needed in the battery management system (BMS) which considers battery SOC and age calculation as affecting parameters.
4. Understanding the Li-ion BESS inverter control interactions and its impacts to the distribution system by means of case studies in an existing smart grid (SSG) in Finland.

2. Study case – Sundom Smart Grid

Sundom Smart Grid (SSG) is represented in Fig. 1, which is a pilot living lab jointly created by ABB, Vaasan Sähköverkko (DSO), Elisa (ICT) and University of Vaasa [26]. Real-time voltage and current measurements (IEC 61850 standard) are sent from the MV distribution network, from all four feeders at HV/MV substation and three MV/LV substations comprising 20 measurement points in total. Measurements are sampled at 80 samples/cycle. In addition, active and reactive power, frequency, RMS voltages, currents etc. measurements are received by Generic Object Oriented Substation Event (GOOSE) messages. SSG doesn't have a Li-ion BESS at the moment, but for study purposes it is added on to the MV distribution network model as shown in Fig. 1.

3. Active network management scheme

Flexible distributed energy resources (DER) in the distribution network (at MV and LV level) plays an important role in providing flexibility services, e.g. as part of distribution network ANM scheme, in the power system for local (DSO) and system-wide (TSO) needs in order to improve grid resiliency and DER (e.g. solar photovoltaic, PV) and electric vehicles (EVs) hosting capacity. These potential flexibility services consist of active (P) and reactive (Q) power control of flexible DER like controllable DG units, energy storages, controllable loads and EVs which are connected to the DSOs network. In this paper, ANM scheme is developed and studied for management of flexibilities in the MV distribution system, particularly focusing on the BESS control design. The developed scheme is then validated in an existing smart grid environment (Sundom Smart Grid). Fig. 2 represents the proposed ANM control architecture proposed in this paper.

BESSs integrated to the SSG MV bus are primarily designed to complement the stochastic nature of wind power generation, i.e., store excess wind power generation and discharge during reduced wind power generation. Secondly, they are used to provide technical ancillary services. These services include management of the voltages (according to grid codes) and improving RES penetration by complementing WTG power generation. Details on the grid codes specifications are explained in [27,28]. The following sub-section explains the development of

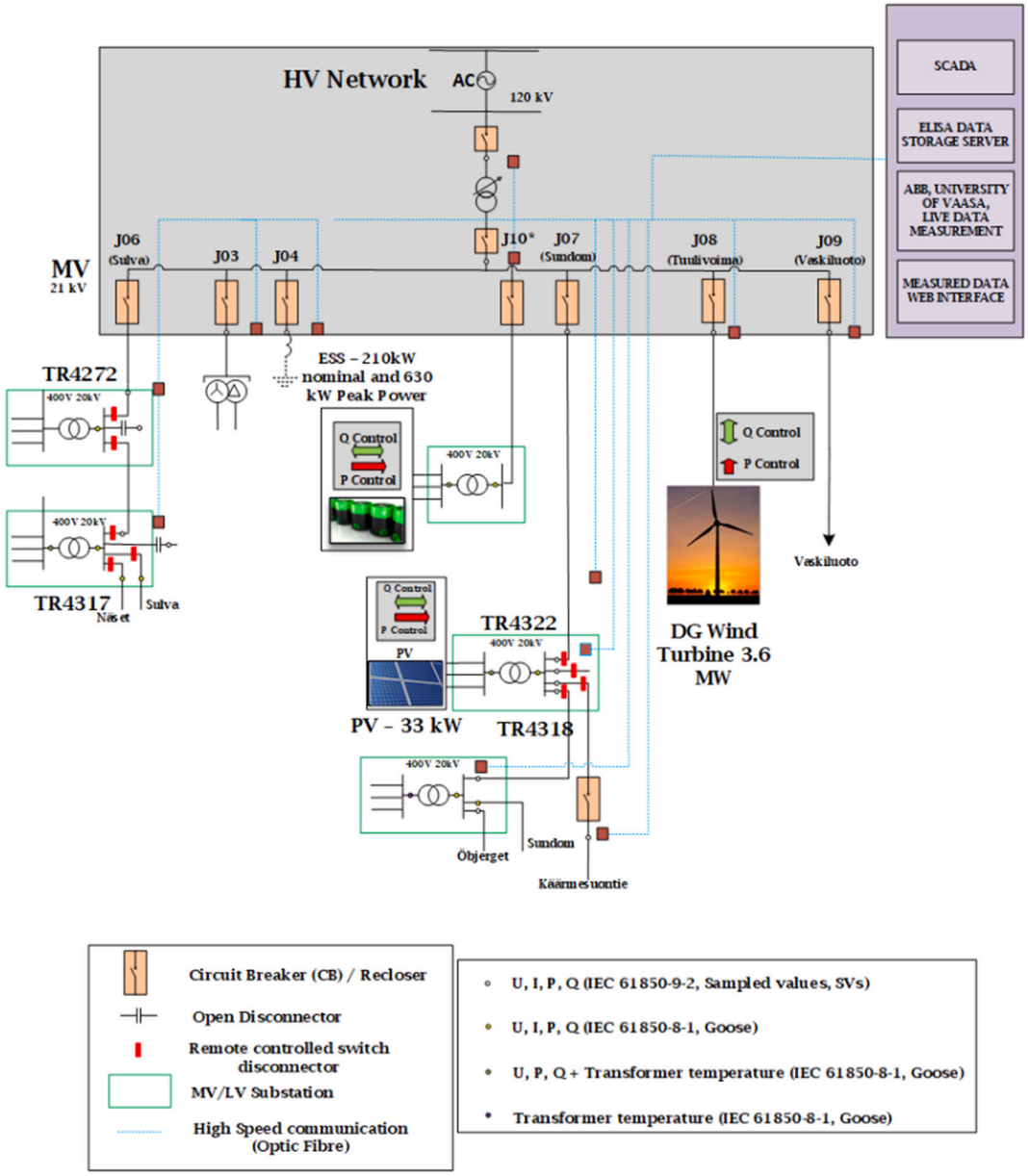

Fig. 1. Sundom Smart Grid network with Li-ion BESS.

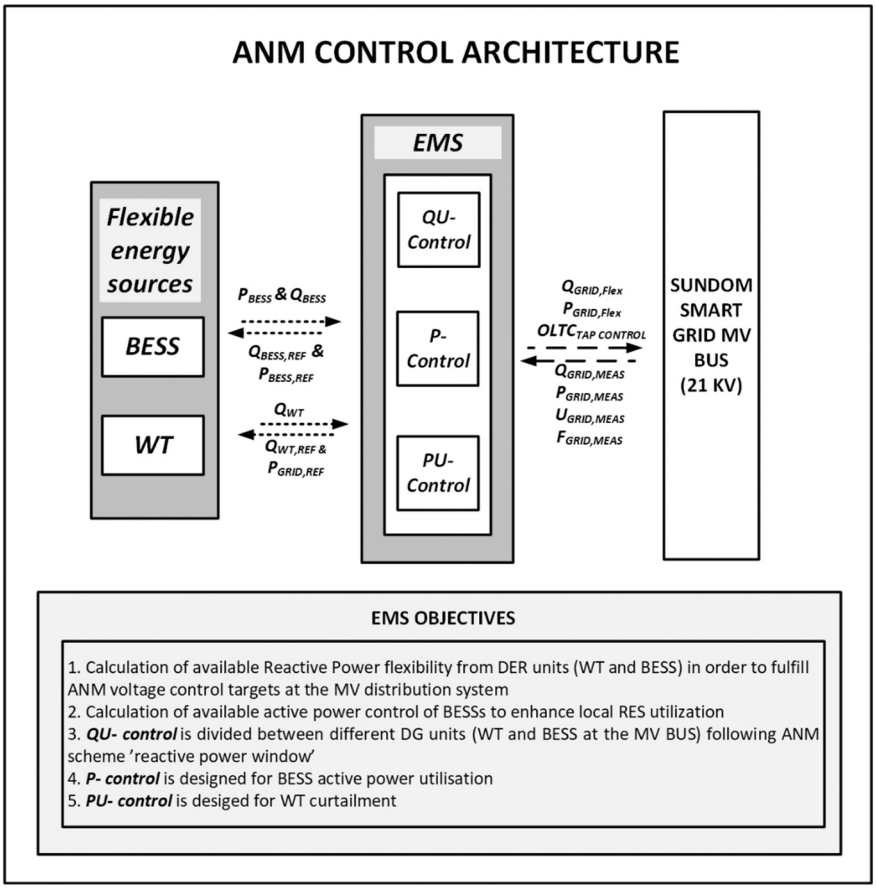

Fig. 2. ANM control architecture.

energy management system (EMS) for providing ANM services, followed battery characterisation and modelling in order to develop elaborate controllers for the Li-ion BESSs.

3.1. Energy management system

Energy management system (EMS) forms the most important block in the overall ANM scheme operations as they provide operational instructions to the flexible energy sources, i.e. in this case Li-ion BESS and WTG. EMS consists of various types of controllers (*QU*-, *P*- and *PU*-controllers) that shall aid in harnessing the flexibilities offered by WTG and Li-ion BESSs. Objective of EMS is to manage Li-ion BESS charge/discharge operations based on WTG active power generation and to keep the voltages in the MV bus within the limits specified by grid codes, by managing available flexibilities in the power system.

3.1.1. P-control

P-control of the EMS is designed for the active power dispatch of Li-ion BESS (P_{BESS}), by controlling charge and discharge operations. The Li-ion BESS has been mostly used to complement wind power generation (P_{WT}) compared to the power demand (P_{Load}). The overall *P*-control layout is shown in Fig. 3. First block, *P*-management system calculates the overall Li-ion BESS active power utilization possibility ($P_{BESS,\ REF}$), by taking P_{Load}, P_{WT} and SOC as inputs and generate $P_{BESS,\ REF}$ as the output. Overall maximum active power discharge expected by the Li-ion BESS is defined by Eq. (1) and that of overall available power for charge is shown in Eq. (2). Eq. (3) generates $P_{BESS,\ REF}$, whose charge and discharge powers are defined by Eqs. (1) and (2) keeping the SOC of the battery within their threshold, SOC_{min} and SOC_{max}. In order to avoid minor deviations by the algorithm in Eq. (3), the charge functionality of the Li-ion BESS has been defined at the SOC lesser than or equal to SOC_{min}. The second block in Fig. 3 corresponds from converting $P_{BESS,\ REF}$ (which corresponds to battery pack power containing *Ns* cells in series to that of *Np* Cells in parallel) to $P_{CELL,\ REF}$ (to active power reference of single cell in the pack) as defined in Eq. (4). This $P_{CELL,\ REF}$ is provided as input to the next block called "Aging aware cell model".

$$P_{dis} = P_{Load} - P_{WT} \tag{1}$$

$$P_{chg} = P_{WT} - P_{Load} \tag{2}$$

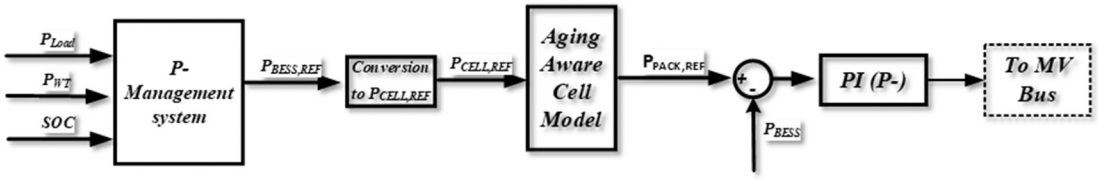

Fig. 3. *P*-control scheme.

$$P_{BESS,REF} = \begin{cases} P_{dis}; (if\ SOC_{min} < SOC < SOC_{max} > and\ P_{Load} > P_{WT}) \\ P_{chg}; (if\ SOC <= SOC_{min} and\ P_{WT} > P_{Load};) \\ 0 \end{cases} \quad (3)$$

$$P_{CELL,REF} = P_{BESS,REF}/Ns*Np \quad (4)$$

The design of aging aware Li-ion battery cell model (third block in Fig. 3) is shown in Fig. 4. $P_{CELL,\ REF}$ is the reference power to address the power system needs per cell in the Li-ion battery pack. This block comprises of battery management system (BMS) which takes $P_{CELL,\ REF}$ as input and calculates SOC by SOC estimation block and the number of completed battery charge/discharge cycles with the help of age calculator block. SOA refers to the calculation of cycle aging or number of completed cycles from the Li-ion battery's charge/discharge currents. Eq. (5) provides details on age calculator design, where the cell power is integrated over period of time and divided by the cell initial cell energy providing the Battery's SOA. SOC is estimated by using coulomb counting method [29], which is shown in Eq. (7). $SOC_{initial}$ stands for the initial SOC of the cell, I_{cell} (t), stands for cell current at time (t) and cell capacity refers to its maximum capacity in Ah. Coulomb Counting method provided the best accuracy with minimal computational effort in an environment where the measurement noise has been minimal, there by generating required inputs for BMS block.

$$SOA = \frac{\int P_{cell}\ dt}{Cell\ Energy} \quad (5)$$

$$P_{CELL,REF,age} = \begin{cases} PP; (if\ P_{CELL,REF} > PP) \\ P_{CELL,REF}; (if\ PP > P_{CELL,REF};) \end{cases} \quad (6)$$

$$\text{SOC} = SOC_{initial} + \frac{\int I_{cell}\ (t)}{Cell\ Capacity}\ dt \quad (7)$$

The BMS functionality houses cell peak power calculation, aging aware battery model and logic based algorithms to limit the cell charge/discharge power within the peak power (PP) limits defined by battery cell aging conditions. The details of the PP characterisation and battery cell modelling are explained in the following sections. The algorithm explaining battery cell power dispatch is as shown Eq. (6), thereby creating a new cell power reference $P_{CELL,\ REF,\ age}$, which now regulates battery cell power always within the PP of the battery cell. By modifying Eq. (4), $P_{BESS,\ REF,\ age}$ is obtained which now provides the battery reference power to the PI-controller, which controls Li-ion BESSs. This $P_{CELL,\ REF,\ age}$ is then provided as the reference to the PI-controller which regulated the Li-ion BESS active power output, P_{BESS}.

3.1.2. QU-control

Reactive power-voltage (*QU*)-control is one of the flexibility services which inverter-based DER can provide, in this study wind turbine generator (WTG) and Li-ion BESS. The limitation of active and reactive power contribution for both these inverter-based sources are explained in detail in [30]. The available reactive power support from WTG is defined as $Q_{wind,\ av}$, and that of Li-ion BESS as $Q_{BESS,\ av}$ *QU*-droop has been designed for *QU*-control as shown in Fig. 5. The droop controller has been designed to have a maximum reactive power (Q_{MAX}) ±2 MVAr. Based on the voltage fluctuation, the droop controller provides the required reactive power reference (Q_{ref}). This Q_{ref}will be satisfied by both WT generator and Li-ion BESS, but prioritising the available reactive from WT first. Eq. (8) defines the reactive power dispatch from WTG and if this reactive power doesn't satisfy Q_{ref}, then reactive power from the Li-ion BESS (Q_{BESS}) will be utilised whose values are defined by Eq. (9).

$$Q_{wind} = \begin{cases} Q_{ref}; (if\ Q_{ref} < Q_{wind,av}) \\ Q_{wind,av}; (if\ Q_{ref} > Q_{wind,av}) \end{cases} \quad (8)$$

$$Q_{BESS} = \begin{cases} Q_{ref} - Q_{wind}; (if\ Q_{ref} > Q_{wind,av}) \\ 0 \end{cases} \quad (9)$$

3.1.3. PU-control

PU-management system is designed to keep in mind the curtailment of renewable energy generation, when the voltage limits exceed 1.05 pu in the MV bus. To manage the curtailment, *PU*-droop control presented in Fig. 6 is utilised for the wind power generation.

3.2. Battery characterisation and aging modelling

Widely adopted battery aging models are based on Arrhenius equation [31,32] that facilitates capturing degradation of battery cells as well due to ambient temperature as an affecting parameter. However, in this paper, we have assumed that the battery systems that are being utilised on the field for stationary grid applications has its own thermal management system that regulates the ambient temperature within a certain range (a constant value) preferred by the operator. Therefore, the aging model been built upon the assumption that the ambient temperature of the battery system shall remain constant when operated for grid applications, typically in room temperatures. It has to be noted that aging model developed in this paper has been based on accelerated aging tests that has been performed at room temperature. Therefore, Li-ion BESS that has been used for ANM applications in this paper, has been assumed to contain a battery thermal management system that is capable of regulating battery ambient temperature at room temperature. The focus of the aging model is to determine evolving PP characteristics due to cycle aging of Li-ion batteries, which has been embedded in control design of Li-ion BESSs.

This section explains the development of PP characterisation models (aging models) and equivalent circuit models utilised in previous section

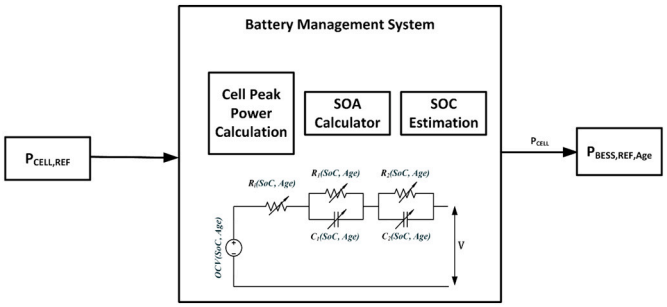

Fig. 4. Aging aware battery cell model.

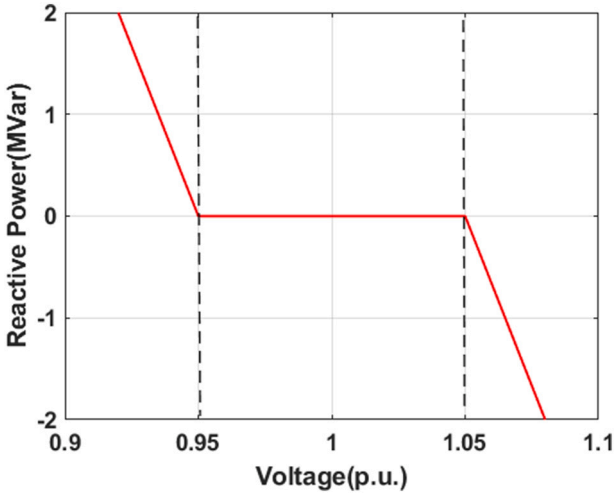

Fig. 5. Proposed *QU*-droop control.

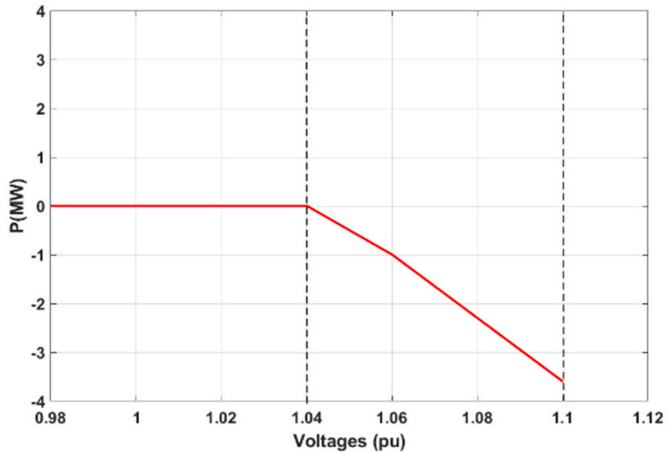

Fig. 6. *PU*-droop settings.

in the development of BMS which forms integral part of the P-controller development for ANM scheme.

3.2.1. Peak power characterisation model

Li-ion BESSs suffer performance degradation due to aging caused by phenomena's such as loss of cycleable lithium ions or active materials, growth of SEI (solid electrolyte interphase) layer, etc. [33], which in turn are a result of calendar and cyclic aging [34,35] of the battery cells. Due to aging, it has been observed that the Li-ion battery capacity reduces and its internal resistance increases, leading to reduction in PP discharge supported by Li-ion BESS. In this study, for development of aging aware Li-ion BESS controllers it is imperative to calculate the PP changes of the battery with aging and SOC. This model will be included in the cell PP calculation block of the BMS. The methodology to extract cell PP changes is explained below.

To calculate the PP changes of Li-ion battery, hybrid pulse power characterisation (HPPC) test based method will be utilised in this study. The HPPC test was performed at 25 °C. At the beginning the cell is fully discharged and fully charged 2 times to measure initial SOC and cell capacity. The HPPC test was performed at 25 °C, at every 10 % SOC step starting from 100 % SOC to 0 % SOC. Prior to pulse sequence, the fully charged were maintained at 100 % SOC and then rested for 1 h. The pulse power sequence consisted of 3C discharge for 10 s, rest at open circuit voltage (OCV) for 3 min, 3C charge for 10 s and rest at OCV for 3 min, followed by partial discharge of 10 % SOC and finally a rest of 1 h. This process was repeated till the battery cell reached 0 % SOC. The aging tests were conducted on the cells at 1C (CCCV charge/ CC discharge) cycling regime and 40 °C ambient temperature. Fig. 7 shows the current profile of the HPPC test performed and Fig. 8 depicts its voltage response for a new cell (i.e. at 0 charge/discharge cycles).

The rationale behind using high current pulse of 3C for 10s has been majorly due to cell characteristics as mentioned by manufacturers' datasheet. This 8 Ah, NMC cell has a continuous maximum discharge C-rate of 2C and its pulsed maximum C-rate has been mentioned as 3C at 10s. Hence, while designing the high current pulse for HPPC test, we chose 3C rate at 10s. This pulse characteristics of the battery cell defines the highest possible current extraction from a particular cell and hence the PP characterisation model has been developed based on this method.

In order to calculate the PP discharge capability of the battery cell at this aging condition, its discharge resistance (R_{dis}) at every high current pulse needs to be calculated. R_{dis} has been computed by Eq. (10), where ΔV_{dis} and ΔI_{dis} are evaluated from the respective voltage and current pulses (see the zoomed images in Figs. 7 and 8). The discharge PP of the Li-ion battery cell has been calculated by Eq. (11), where the OCV and V_{min} are evaluated from the voltage response of the HPPC test. By repeating this at every 10 % step SOC, the overall PP profile at different depths of discharge (DODs) at one particular aging condition. In the aging test performed in this study, the HPPC test profile has been run at the intervals of specified by number of cycles, i.e. at 0, 500, 800, 1200 and 1600 cycles. PP discharge of the Li-ion NMC battery cell has been evaluated with the help of HPPC test profiles obtained at different aging conditions. Fig. 9 depicts the PP output of the Li-ion cell at different aging levels, which were calculated with the help of Eqs. (10) and (11). Similarly, charge PPs were calculated with the help of Eqs. (12) and (13), which is represented by Fig. 10. A script was written in Matlab/ Simulink interface for this purpose. The calculated PP values were then stored in a two-dimensional lookup table whose output will be controlled by SOC and aging parameters and then integrated to the BMS control block.

$$R_{dis} = \frac{\Delta V_{dis}}{\Delta I_{dis}} = \frac{V_{t1} - V_{t10}}{I_{t1} - I_{t10}} \tag{10}$$

$$PP_{Dis} = \frac{V_{min}{}^{*}(OCV - V_{min})}{R_{dis}} \tag{11}$$

$$R_{cha} = \frac{\Delta V_{cha}}{\Delta I_{cha}} = \frac{V_{t1} - V_{t10}}{I_{t1} - I_{t10}} \tag{12}$$

$$PP_{cha} = \frac{V_{min}{}^{*}(OCV - V_{maz})}{R_{cha}} \tag{13}$$

3.2.2. Equivalent circuit battery model

Li-ion battery model capable of emulating its performance at different SOC and age intervals forms the second requirement for BMS design and development. For this purpose, second order equivalent circuit model (SOEC) based on Thevenin's circuit model [36] representing the dynamic response of the Lithium-ion battery including its

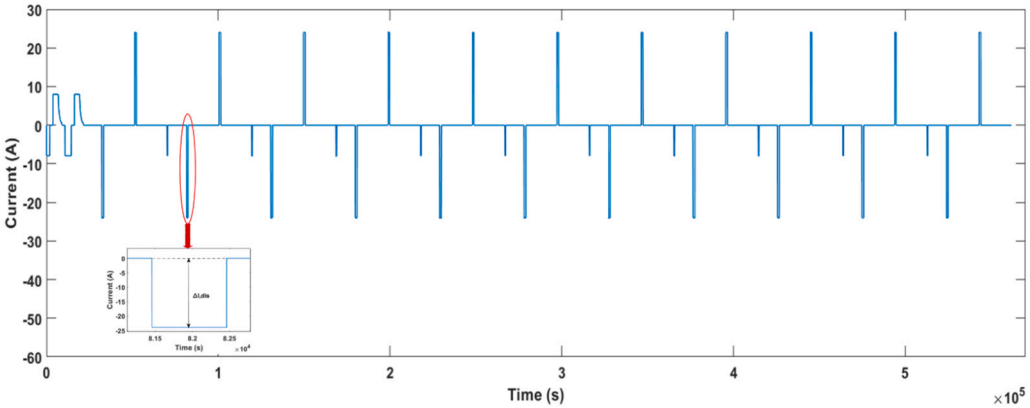

Fig. 7. HPPC current pulse profile.

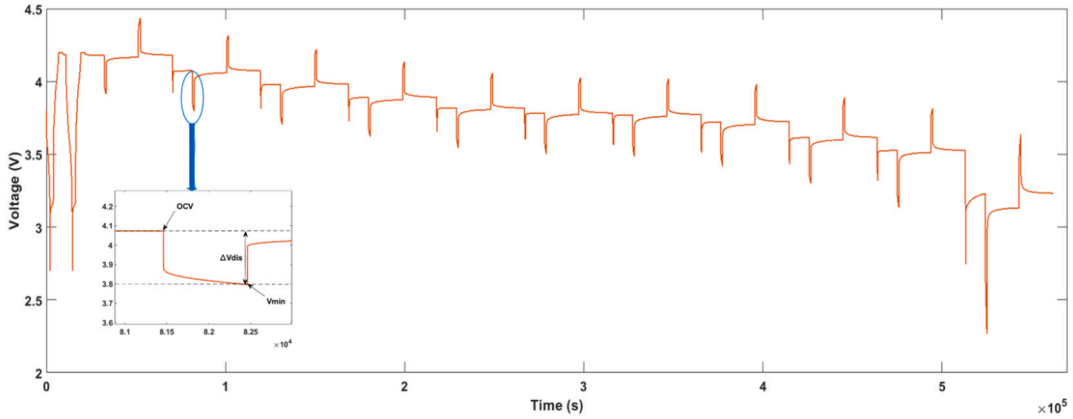

Fig. 8. HPPC voltage response.

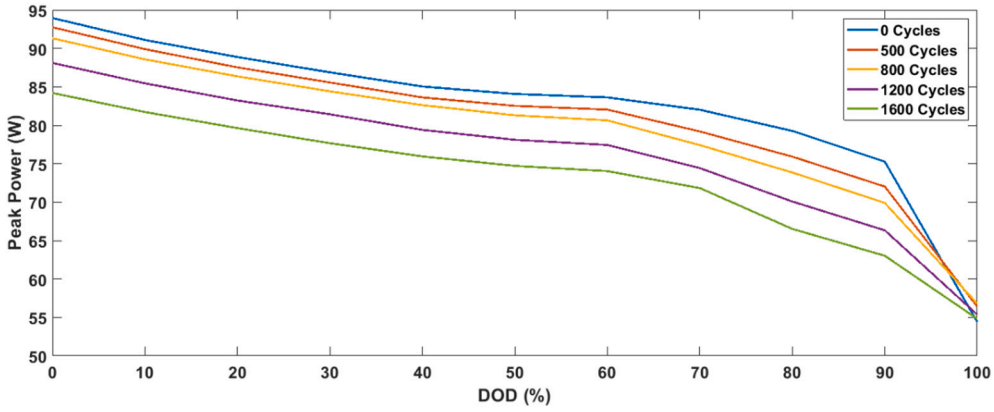

Fig. 9. Discharge peak power of Li-ion battery cell at different aging intervals.

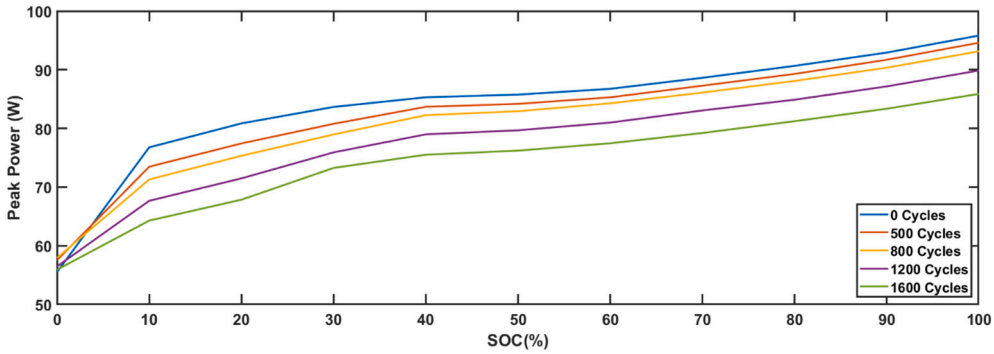

Fig. 10. Charge peak power of Li-ion battery cell at different aging intervals.

performance affecting parameters such as SOC, current-rate (C-rate) and battery age has been chosen. SOEC model denotes the processes occurring inside the battery cell such as charge transfer, diffusion and solid electrolyte interface (SEI) layer in the form of resistors and capacitors.

Fig. 11 shows the proposed dynamic SOEC for the NMC battery cell. OCV is modelled as an ideal voltage source, and the internal resistance is modelled as R_i. Two RC combinations are suggested for modelling Li-ion battery cell, so that the dynamic behaviour is modelled as R_1, C_1, R_2 and C_2. The model parameters (OCV, R_i, R_1, C_1, R_2 and C_2) are obtained by HPPC tests [37], i.e. the HPPC tests were run at different SOC's (from 0 % to 100 % at 10 % intervals) and at different aging intervals (i.e. at 0, 500, 800, 1200 and 1600 cycles of operation). The battery cell cycle aging test was performed at 1C charge/discharge rate and 25 °C [37]. A

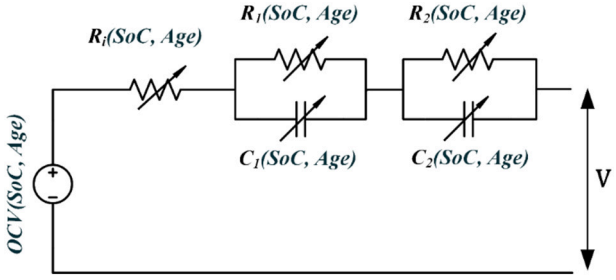

Fig. 11. Proposed second order equivalent circuit model

Matlab script was developed to calculate the measurements of SOEC parameters from HPPC test voltage response (Fig. 8) repeated for all the HPPC curves (i.e at all the aging intervals).

4. Case study evaluation

SSG network (explained in Section 2) has been the power system under study to access the developed ANM scheme and its operations to manage MV voltage stability and boosting renewable power penetration by neat utilization of Li-ion BESSs. It is important to simulate the power system over a long period of time (hours to few days), in order to validate the effectiveness of the designed ANM secondary controllers (*P*-, *QU*-, and *PU*-controllers) and verify the setpoints provided to them. The control setpoints for Li-ion BESS have considered their aging as an affecting parameter in the control loop. Such large scale and longer time horizon power system simulations are computationally demanding and in order to perform accurate analysis, real-time simulations provide an avenue for quick and efficient approach. In the developed ANM scheme, the role of Li-ion BESS active power dispatch is to enhance wind power generation and reactive power flexibilities from WTG and Li-ion BESS is to manage MV distribution system voltage. The simulation models for these studies are developed in ePhasorSim platform by OPAL-RT, details of which are explained in [30].

The real-time simulation environment is presented in Fig. 12. The power system model of the modified SSG with Li-ion BESS in MV distribution system explained in Section 2. The power system model is based on the system parameters of the SSG provided by the local DSO and that of power generation details from WTG are based on the actual site data. The details of the power system model is similar to the previous studies undertaken by the authors [30,38], except the change in battery model which includes their aging characteristics and the Li-ion BESS controllers whose power outputs are governed by their aging aware PP capability. It has to be noted that in this simulation model services from the on-line tap changer (OLTC) transformer wasn't available, reason being to study management of flexibilities from available sources. The major objective of this study is to analyse how battery aging affects its charge/discharge power output and their impact on ANM operations in SSG. Case studies are defined in the following section to conduct these analyses.

4.1. Case 1: base case (non-active ANM scheme)

In this case, SSG is simulated without flexibilities from BESS and WTG operating in the MV distribution system, which is considered as the base case study. The simulations are performed for a period of 3 days with a time step of 1 s. This approach enables us to record the active and reactive power flows and the voltage measurements at various MV buses in the power system without any ANM being active. The SSG WTG is of permanent magnet synchronous generator (PMSG) type and connected to grid by full-power converter, thereby allowing it to absorb or inject reactive power to 100 % of its rated power. In this case, the reactive power control (*QU*-control) of the WTG is disabled, to record the original characteristics in the SSG without the operation of any flexible energy resources adhering to IEEE 1547–2018 [39] guidelines.

Fig. 13 shows the voltages at various MV buses whose values are seen to be between 0.94 and 0.95 p.u. The active power generation from WTG for 3 days is recorded in Fig. 14(a) and (b) provides details on reactive power contribution from WTG and Li-ion BESSs.

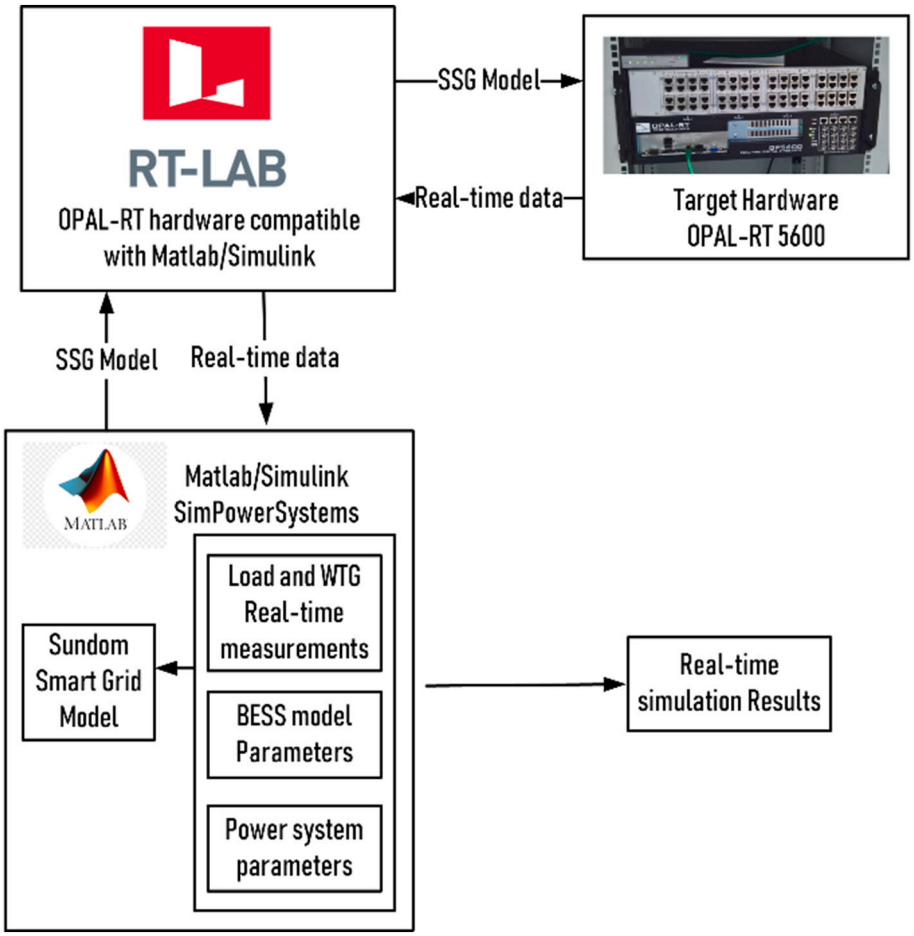

Fig. 12. Real-time simulation setup.

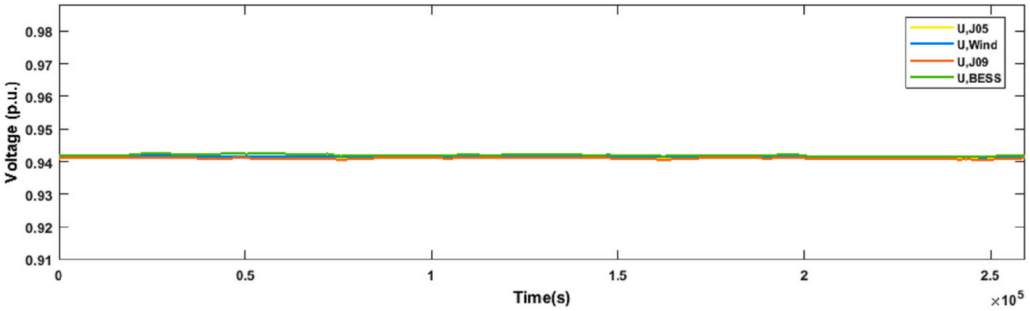

Fig. 13. MV bus voltages in SSG (Case 1 simulation results).

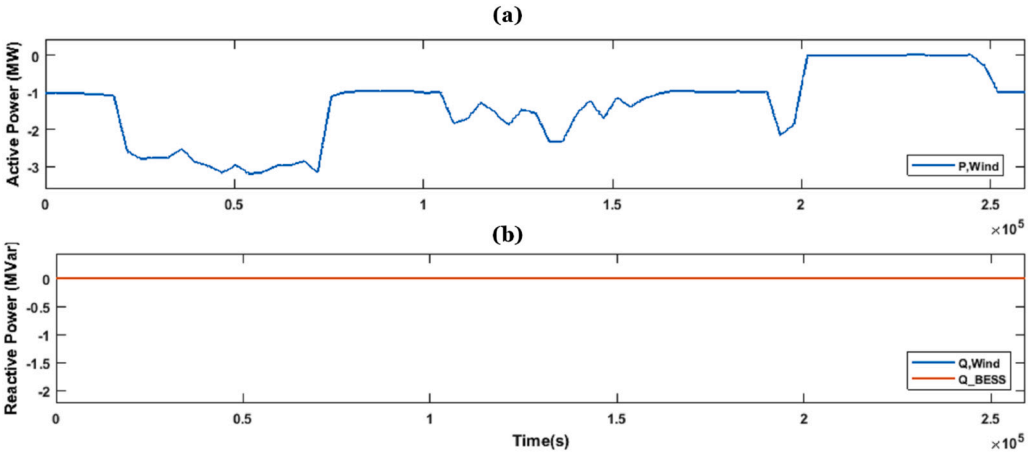

Fig. 14. (a) WTG power generation; (b) reactive power contribution from WTG and Li-ion BESS (Case 1 simulation results).

4.2. Case 2: active ANM scheme and new Li-ion BESS (at 0 cycles of operation)

The effect of proposed ANM scheme and the amount of power and energy a new Li-ion BESS (i.e. at 0 cycles of operation), can support the $P_{BESS,REF}$ generated by Eq. (3). The *QU*-secondary control comes into effect along with the *P*-control to manage voltage regulation and complement wind power generation. Fig. 14(a) in previous case represents the active power generation of WTG, which is unchanged. Fig. 15 shows the amount of reactive power services offered by *QU*-control which is satisfied by Q_{Wind} alone. Quite much (closer to 1.5 MVAr) reactive power feeding is required for voltage compensation, this is due to the fact that WTG is almost directly connected to the HV/MV substation MV bus (which makes it a very stiff connection point from voltage effect point of view). The *QU*-controller does not need reactive power services from Li-ion BESS in this case. Based on the *QU*-controller's operation, the voltages at various buses of MV distribution system are seen to improve (0.95 p.u. and above) and fall within the purview of conditions provided by grid codes as described in Fig. 16. Hence, proposed ANM scheme satisfies its first objective.

Fig. 17 represents the Li-ion BESS active power charge and discharge characteristics. The blue line in in Fig. 17 corresponds to the overall available charge and discharge power ($P_{BESS,REF}$) based on Eq. (3) and that of red line corresponds to the actual charge and discharge power (P_{BESS}), dispatched to and from the Li-ion BESS. In this case, the Li-ion battery is considered as new system without any cycles of charge and discharge. Comparing $P_{BESS,REF}$ and P_{BESS} it is evident that the *P*-control (which considers SOC and age as its input) works as desired by keeping the battery charge and discharge power within the maximum possible threshold. It can also be observed that the $P_{BESS,REF}$ has lower power and lower DODs (i.e. the cycles in the middle of Fig. 6) and can be entirely satisfied by P_{BESS}.

Fig. 18(a) represents the SOC of Li-ion BESS which as committed, cycles between 10 % and 90 % SOC and Fig. 18(b) shows the total number of charge/discharge cycles accumulated in a period of 3 days. The major objective of this study was to validate the design and operation of secondary controllers (*QU*- and *P*-controllers), which allows enforcement of the ANM scheme which has now been verified for a new Li-ion BESS.

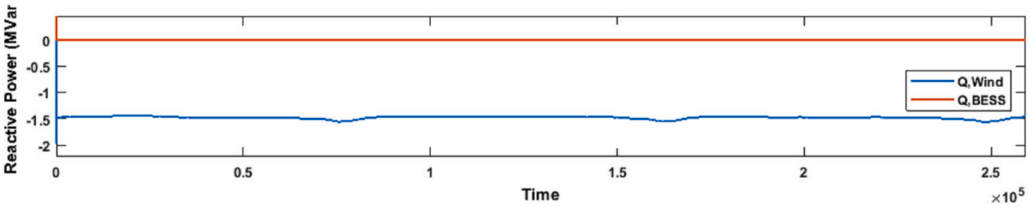

Fig. 15. Reactive power contribution from WTG and Li-ion BESS (Case 2 simulation results).

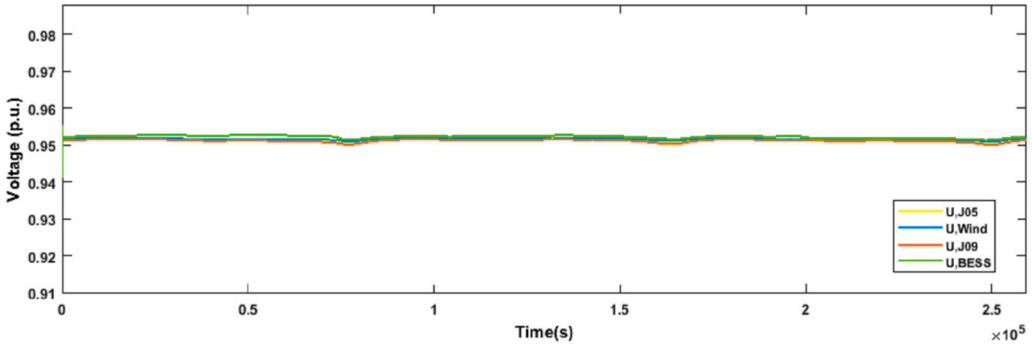

Fig. 16. MV bus voltages in SSG (Case 2 simulation results).

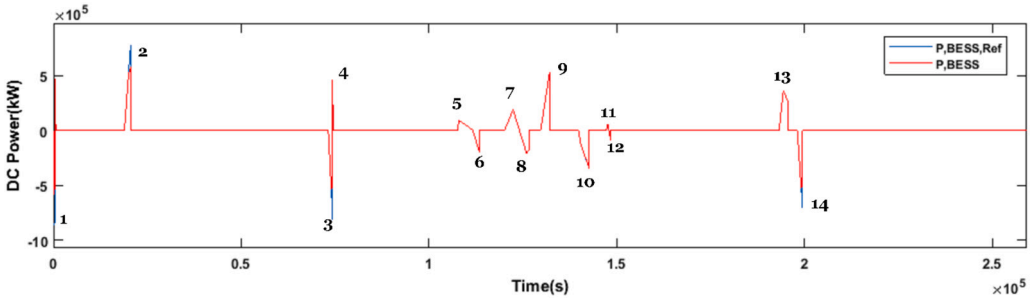

Fig. 17. Li-ion BESS active power reference and actual power dispatch for new cells (Case 2 simulation results).

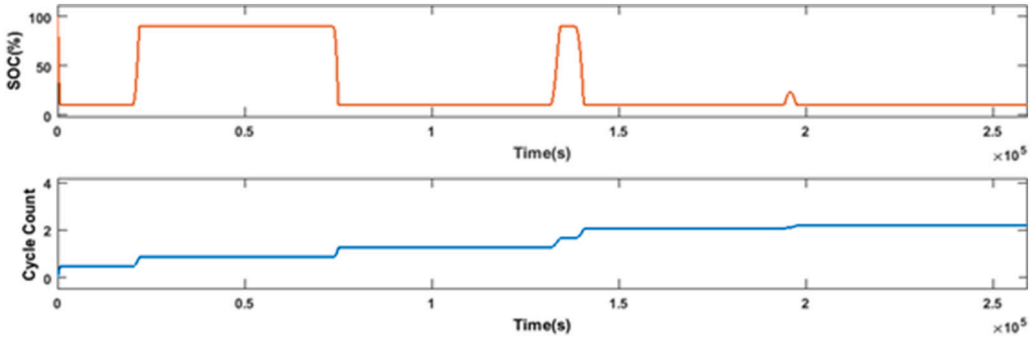

Fig. 18. (a) Li-ion BESS SOC and (b) Battery cycle count of operation (Case 2 simulation results)

4.3. Case 3: active ANM scheme and used Li-ion BESS (after 1200 cycles of operation)

Objective of this case to understand the impact of Li-ion BESS aging on its performance, particularly the peak load it can support. In this simulation case, the Li-ion BESS has been considered to have undergone considerable aging, i.e. about 1200 cycles of charge/discharge operations.

Fig. 19 shows the amount of reactive power services offered by *QU*-control, which is satisfied by Q_{Wind} alone, even in this case with aged Li-ion BESS. The voltages in the MV distribution system are seen to be within the threshold values defined by grid codes as seen in Fig. 20. However, the active power characteristics which is based on the aging aware *P*-control of Li-ion BESS provides a different picture on actual active power discharge. Compared to Fig. 17, in Fig. 21 the actual peak active power of the Li-ion BESS has been modified based on the age related controller. The PP outputs are observed to be lesser in magnitude where the cycles are deep with higher DOD and $P_{BESS,REF}$. Table I

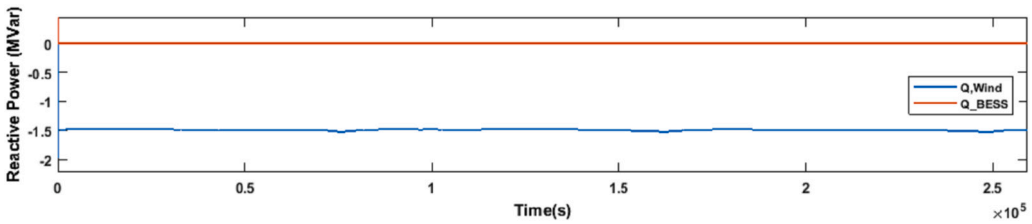

Fig. 19. Reactive power contribution of WTG and Li-ion BESS (Case 3 simulation results).

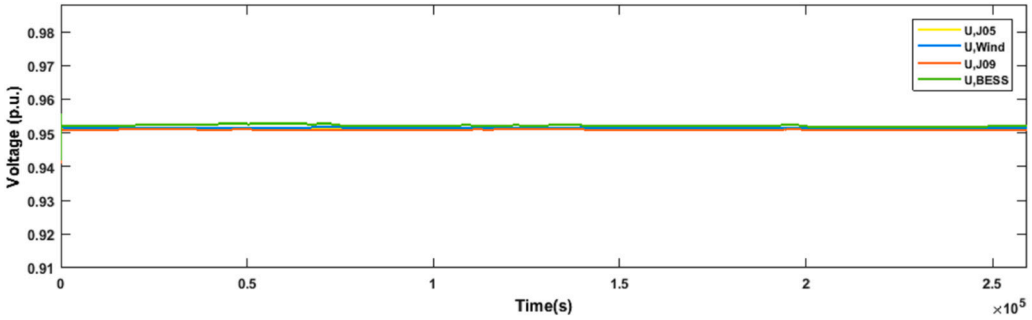

Fig. 20. MV bus voltages (Case 3 simulation results).

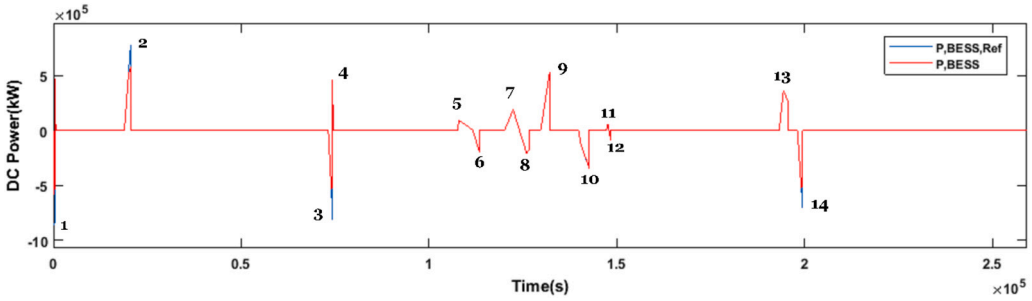

Fig. 21. Li-ion BESS active power reference and actual power dispatch for aged cells (Case 3 simulation results).

provides comparison in active power changes of Li-ion BESS, which shows that cycles 1,2,3 and 14 which has higher power levels compared to other pulses and $P_{BESS,REF}$ are seen to have a dip in the PP dispatch. This is due to the *P*-control characteristics, which tends to lower PP of Li-ion BESS with aging (Table 1).

5. Conclusion

The application of Li-ion BESS in this work has been for active network management (ANM) of distribution grids and to improve renewable energy penetration and utilization in smart grids. The ANM scheme is designed to maintain the distribution system stable within the limits defined by the grid codes by tapping the flexibility services (both active and reactive power related flexibility services) offered by flexible energy sources.

However, the Li-ion battery tends to age with usage causing degradation in their performance characteristics that in turn lead to reduction in their PP charge/discharge capability. This change in PP provisioning of the Li-ion BESS needs to be captured in the secondary control layer of the active network management scheme, as the power dispatch in this control layer are typically of higher DODs and power ratings compared to the primary control layer.

For that reason, an age (for Li-ion BESS) influenced adaptive *P*-control layer (secondary control layer) in the ANM has been proposed in this study, which considers the operational battery SOA (number of completed charge/discharge cycles) as input to the control system. The battery management system (within *P*-control layer), consists of an accurate second order equivalent circuit Li-ion battery model that generates accurate voltage, power and energy characteristics of the Li-ion battery cell, considering battery SOC and SOH as its affecting parameters. The BMS also hosted the PP calculation algorithm, which provides the PP reference of the battery cell at all instances of SOH. The overall objective of *P*-control layer has been to generate the Li-ion BESS active power reference which is within the threshold of battery charge/discharge PP capability, which is defined by its SOH and provided by PP calculation algorithm. Thereby, solving the problem of managing the battery charge/discharge operations always within the threshold of their peak active power performance.

Based on the simulation studies results, it can be noted that the designed EMS controllers acted as required to provide flexibilities to manage system voltages within the threshold defined by grid codes. Despite aging aware control of Li-ion BESS using *P*-controller of the EMS, it can be observed that the voltages were maintained within the threshold defined by grid codes by the *QU*-controller. It can also be observed that the cycles with higher power discharge and DOD showed the influence of battery aging by reduced power dispatch with aging and the cycles with lower power discharge and DODs had no impacts of battery aging on their power dispatch.

Table 1
Li-ion BESS PP dispatch comparison.

Cycle number	Case 2: new Li-ion BESS active power dispatch (kW)	Case 3: aged Li-ion BESS active power dispatch (kW)
1	−631,4	−559,2
2	603,7	561,8
3	−556,4	−519,7
4	438,5	438,5
5	174,6	174,6
6	−282,7	−282,7
7	264,1	264,1
8	−310,4	−310,4
9	478,7	478,7
10	−345,9	−345,9
11	44,4	44,4
12	−52,1	−52,1
13	183,7	183,7
14	−537,1	−515,9

6. Future studies

Li-ion battery aging is an irreversible phenomenon which leads to permanent degradation of its performance parameters, i.e., its capacity and power dispatch characteristics in particular. These degradation parameters must be considered, especially while developing battery controllers and various other technical studies involving Li-ion batteries

such as techno-economic analyses, battery sizing and determining their optimum location in the power system. Therefore, the future research directions are multi-fold in nature. The main ones are listed below:

1. Impact of battery aging shall be studied in detail by development of aging aware adaptive controllers in their secondary and tertiary control layers, for various applications that require higher power charging and discharging at higher DODs. The comparison between adaptive and non-adaptive *P*-control on the aging rate and safety aspects of Li-ion BESSs needs to be analysed experimentally, which is of interest for future research.
2. The size and location in the power grid of Li-ion BESS in a power system is highly influenced by its technical performance and aging characteristics [40–42]. Therefore, determination of optimal size and location of Li-ion BESS based on their performance characteristics, including its aging characteristics has been considered for future research.
3. Due to the changing PP characteristics of Li-ion BESSs due to aging, techno-economic analysis of Li-ion BESS participation has to include their aging characteristics and this forms another interest towards future studies, where scheduling of Li-ion BESSs shall drastically change with aging.

CRediT authorship contribution statement

Chethan Parthasarathy: Conceptualization, Methodology, Software, Validation, Formal analysis, Investigation, Writing – original draft, Visualization. **Hannu Laaksonen:** Writing – review & editing, Supervision, Project administration, Funding acquisition. **Eduardo Redondo-Iglesias:** Writing – review & editing, Methodology, Validation. **Serge Pelissier:** Writing – review & editing, Methodology, Validation.

Declaration of competing interest

The authors declare that they have no known competing financial interests or personal relationships that could have appeared to influence the work reported in this paper.

Data availability

The data that has been used is confidential.

References

[1] Y. Yang, S. Bremner, C. Menictas, M. Kay, Battery energy storage system size determination in renewable energy systems: a review, Renew. Sust. Energ. Rev. 91 (March) (Aug. 2018) 109–125.

[2] S.Bin Wali, et al., Battery storage systems integrated renewable energy sources: a biblio metric analysis towards future directions, J. Energy Storage 35 (November 2020) (2021) 102296.

[3] O. Palizban, K. Kauhaniemi, J.M. Guerrero, Microgrids in active network management - part I: hierarchical control, energy storage, virtual power plants, and market participation, Renew. Sust. Energ. Rev. 36 (2014) 428–439.

[4] O. Palizban, K. Kauhaniemi, J.M. Guerrero, Microgrids in active network management - part II: system operation, power quality and protection, Renew. Sust. Energ. Rev. 36 (2014) 440–451.

[5] G. Rancilio, A. Rossi, C. Di Profio, M. Alborghetti, A. Galliani, M. Merlo, Grid-scale BESS for ancillary services provision: SoC restoration strategies, Appl. Sci. 10 (12) (2020) 1–18.

[6] M. Mahesh, D.V. Bhaskar, T.N. Reddy, P. Sanjeevikumar, J.B. Holm-Nielsen, Evaluation of ancillary services in distributiogrid using large-scale battery energy storage systems, IET Renew. Power Gener. 14 (19) (2020) 4216–4222.

[7] C. Parthasarathy K. Sirviö H. Hafezi H. Laaksonen , "Modelling Battery Energy Storage Systems for Active Network Management – Coordinated Control Design and Validation," IET Renew. Power Gener., pp. 1–10.

[8] D. Choi, et al., Li-ion battery technology for grid application, J. Power Sources 511 (July) (2021), 230419.

[9] H.C. Hesse, M. Schimpe, D. Kucevic, A. Jossen, Lithium-ion battery storage for the grid - a review of stationary battery storage system design tailored for applications in modern power grids vol. 10, no. 12, 2017.

[10] L. Cai, N.F. Thornhill, S. Kuenzel, B.C. Pal, A test model of a power grid with battery energy storage and wide-area monitoring, IEEE Trans. Power Syst. 34 (1) (2019) 380–390.

[11] W. Liu, Y. Xu, X. Feng, Y. Wang, Optimal fuzzy logic control of energy storage systems for V/f support in distribution networks considering battery degradation, Int. J. Electr. Power Energy Syst. 139 (July) (2021) 2022.

[12] A.M. Shotorbani, B. Mohammadi-Ivatloo, L. Wang, S. Ghassem-Zadeh, S. H. Hosseini, Distributed secondary control of battery energy storage systems in a stand-alone microgrid, IET Gener. Transm. Distrib. 12 (17) (Sep. 2018) 3944–3953.

[13] L. Zhang, et al., Improved cycle aging cost model for battery energy storage systems considering more accurate battery life degradation, IEEE Access 10 (2022) 297–307.

[14] K. Liu, et al., Electrochemical modeling and parameterization towards control-oriented management of lithium-ion batteries, Control. Eng. Pract. 124 (Jul. 2022), 105176.

[15] X. Jin, Aging-aware optimal charging strategy for lithium-ion batteries: considering aging status and electro-thermal-aging dynamics, Electrochim. Acta 407 (Mar. 2022), 139651.

[16] Y.R. Lee, H.J. Kim, M.K. Kim, Optimal operation scheduling considering cycle aging of battery energy storage systems on stochastic unit commitments in microgrids, Energies 14 (2) (Jan. 2021) 470.

[17] M. Abogaleela, K. Kopsidas, Battery energy storage degradation impact on network reliability and wind energy curtailments, in: 2019 IEEE Milan PowerTech 2019, PowerTech, 2019, pp. 1–6.

[18] D. Kirli, A. Kiprakis, Techno-economic potential of battery energy storage systems in frequency response and balancing mechanism actions, J. Eng. 2020 (9) (2020) 774–782.

[19] Y. Li, et al., Design of minimum cost degradation-conscious lithium-ion battery energy storage system to achieve renewable power dispatchability, Appl. Energy 260 (November 2019) (2020) 114282.

[20] Y. Li, M. Vilathgamuwa, S.S. Choi, T.W. Farrell, N.T. Tran, J. Teague, Development of a degradation-conscious physics-based lithium-ion battery model for use in power system planning studies, Appl. Energy 248 (May) (2019) 512–525.

[21] J.M. Reniers, G. Mulder, S. Ober-Blöbaum, D.A. Howey, Improving optimal control of grid-connected lithium-ion batteries through more accurate battery and degradation modelling, J. Power Sources 379 (January) (2018) 91–102.

[22] A. Allahham, D. Greenwood, C. Patsios, P. Taylor, Adaptive receding horizon control for battery energy storage management with age-and-operation-dependent efficiency and degradation, Electr. Power Syst. Res. 209 (Aug. 2022), 107936.

[23] D.J. Ryan, R. Razzaghi, H.D. Torresan, A. Karimi, B. Bahrani, Grid-supporting battery energy storage systems in islanded microgrids: a data-driven control approach, IEEE Trans. Sustain. Energy 12 (2) (Apr. 2021) 834–846.

[24] R. Zhao, R.D. Lorenz, T.M. Jahns, Lithium-ion battery rate-of-degradation modeling for real-time battery degradation control during EV drive Cycle, in: 2018 IEEE Energy Convers.Congr. Expo. ECCE2018, Dec. 2018, pp. 2127–2134.

[25] N. Tian, H. Fang, Y. Wang, Real-time optimal lithium-ion battery charging based on explicit model predictive control, IEEE Trans. Ind. Informa. 17 (2) (Feb. 2021) 1318–1330.

[26] H. Laaksonen, Future-proof islanding detection schemes in Sundom smart grid, Cired 2017 (June) (2017) 12–15.

[27] H. Laaksonen, C. Parthasarathy, H. Khajeh, M. Shafie-Khah, N. Hatziargyriou, Flexibility services provision by frequency-dependent control of on-load tap-changer and distributed energy resources, IEEE Access 9 (2021) 45587–45599.

[28] C. Parthasarathy H. Laaksonen , "Control and Co-ordination of Flexibilities for Active Network Management in Smart Grids – Li-ion BESS Fast Charging Case.".

[29] J. Meng, G. Luo, M. Ricco, M. Swierczynski, D.-I. Stroe, R. Teodorescu, Overview of lithium-ion battery modeling methods for state-of-charge estimation in electrical vehicles, Appl. Sci. 8 (5) (2018) 659.

[30] C. Parthasarathy, K. Sirviö, H. Hafezi, H. Laaksonen, Modelling battery energy storage systems for active network management—coordinated control design and validation, IET Renew. Power Gener. 15 (11) (Aug. 2021) 2426–2437.

[31] G. Kucinskis, M. Bozorgchenani, M. Feinauer, M. Kasper, M. Wohlfahrt-Mehrens, T. Waldmann, Arrhenius plots for Li-ion battery ageing as a function of temperature, C-rate, and state of health – an experimental study, J. Power Sources 549 (September) (2022), 232129.

[32] J. Teh, Uncertainty analysis of transmission line end-of-life failure model for bulk electric system reliability studies, IEEE Trans. Reliab. 67 (3) (2018) 1261–1268.

[33] B. Xu, A. Oudalov, A. Ulbig, G. Andersson, D.S. Kirschen, Modeling of lithium-ion battery degradation for cell life assessment, IEEE Trans. Smart Grid 9 (2) (2018) 1131–1140.

[34] R. Xiong, Y. Pan, W. Shen, H. Li, F. Sun, Lithium-ion battery aging mechanisms and diagnosis method for automotive applications: recent advances and perspectives, Renew. Sust. Energ. Rev. 131 (Oct. 2020), 110048.

[35] X. Lai, et al., Critical review of life cycle assessment of lithium-ion batteries for electric vehicles: a lifespan perspective, eTransportation 12 (May 2022), 100169.

[36] S. Nejad, D.T. Gladwin, D.A. Stone, A systematic review of lumped-parameter equivalent circuit models for real-time estimation of lithium-ion battery states, J. Power Sources 316 (2016) 183–196.

[37] R. Arunachala, C. Parthasarathy, A. Jossen, J. Garche, Inhomogeneities in large format lithium ion cells: a study by battery modelling approach, ECS Trans. 73 (1) (2016) 201–212.

[38] C. Parthasarathy, H. Hafezi, H. Laaksonen, Integration and control of lithium-ion BESSs for active network management in smart grids: Sundom smart grid backup feeding case, Electr. Eng. 104 (2) (Apr. 2022) 539–553.

[39] IEEE Standard Association, IEEE Std. 1547-2018. Standard for Interconnection And Interoperability of Distributed Energy Resources With Associated Electric Power Systems Interfaces, 2018.
[40] H. Alsharif, M. Jalili, K.N. Hasan, Power system frequency stability using optimal sizing and placement of battery energy storage system under uncertainty, J. Energy Storage 50 (April) (2022), 104610.
[41] Y. Yang, S. Bremner, C. Menictas, M. Kay, Battery energy storage system size determination in renewable energy systems: a review, Renew. Sust. Energ. Rev. 91 (January) (2018) 109–125.
[42] M.K. Metwaly, J. Teh, Optimum network ageing and battery sizing for improved wind penetration and reliability, IEEE Access 8 (2020) 118603–118611.